Figure S1, related to Figure 1 (Franco, et. al.)

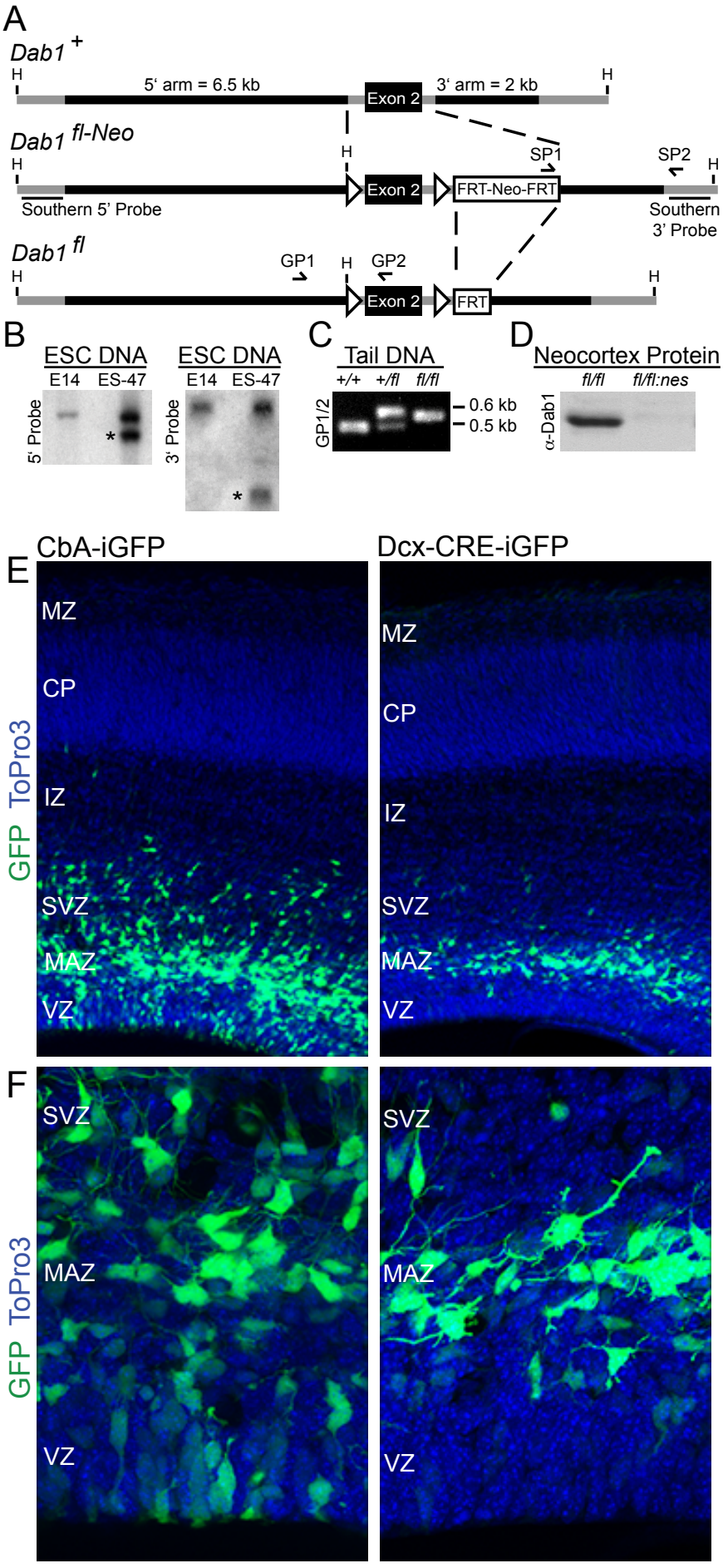

Figure S1. (A-D) Generation and characterization of a conditional Dab1 allele. **(A)** Schematic diagram of wild-type (+) and floxed (*fl-Neo, fl*) alleles of the *Dab1* gene. Thick black bars represent DNA segments used for constructing the targeting vector; gray bars identify flanking genomic DNA. Relevant restriction sites (H, HindIII), Southern probes (thin black bars) and PCR primers for screening (SP1, SP2) and genotyping (GP1, GP2) are indicated. **(B)** Southern blot analysis of targeted ES cells. Genomic DNA from wild-type (E14) and targeted (ES-47) ES cells was digested with HindIII and hybridized with 5’ and 3’ external probes. Star (*) indicates the targeted *fl-Neo* allele. **(C)** PCR analysis of floxed *Dab1* mice. Genomic DNA from wild-type, heterozygous and homozygous *Dab1-fl* mouse tails was analyzed using genotyping primers GP1 and GP2. **(D)** Loss of Dab1 protein upon CNS-wide expression of CRE recombinase from the *Nestin-CRE* transgene. Representative immunoblot of neocortical tissue from E16.5 homozygous *Dab1-fl* mice without (*fl/fl*) or with (*fl/fl;nes*) the *Nestin-CRE* transgene. **(E-F)** Neuron-specific expression from the *Dcx* promoter after *in utero* electroporation. **(E)** Wild-type embryos were electroporated at E14.5 and analyzed at E16.5. Left panel, cortical sections from embryos electroporated with a plasmid in which EGFP is expressed constitutively from the chicken β-actin promoter (CbA). Right panel, coronal sections from embryos electroporated with Dcx-CRE-iGFP in which Cre and EGFP are expressed from a mouse doublecortin promoter fragment. Sections are counterstained with ToPro3 to reveal cortical cytoarchitecture. Note the absence of GFP expression in the VZ with Dcx-CRE-iGFP compared to CbA-iGFP. **(F)** Higher magnification of the VZ from images shown in **(E)**. CP, cortical plate; IZ, intermediate zone; MAZ; multipolar accumulation zone; MZ, marginal zone; SVZ, subventricular zone; VZ, ventricular zone.

Figure S2, related to Figure 2 (Franco, et. al.)

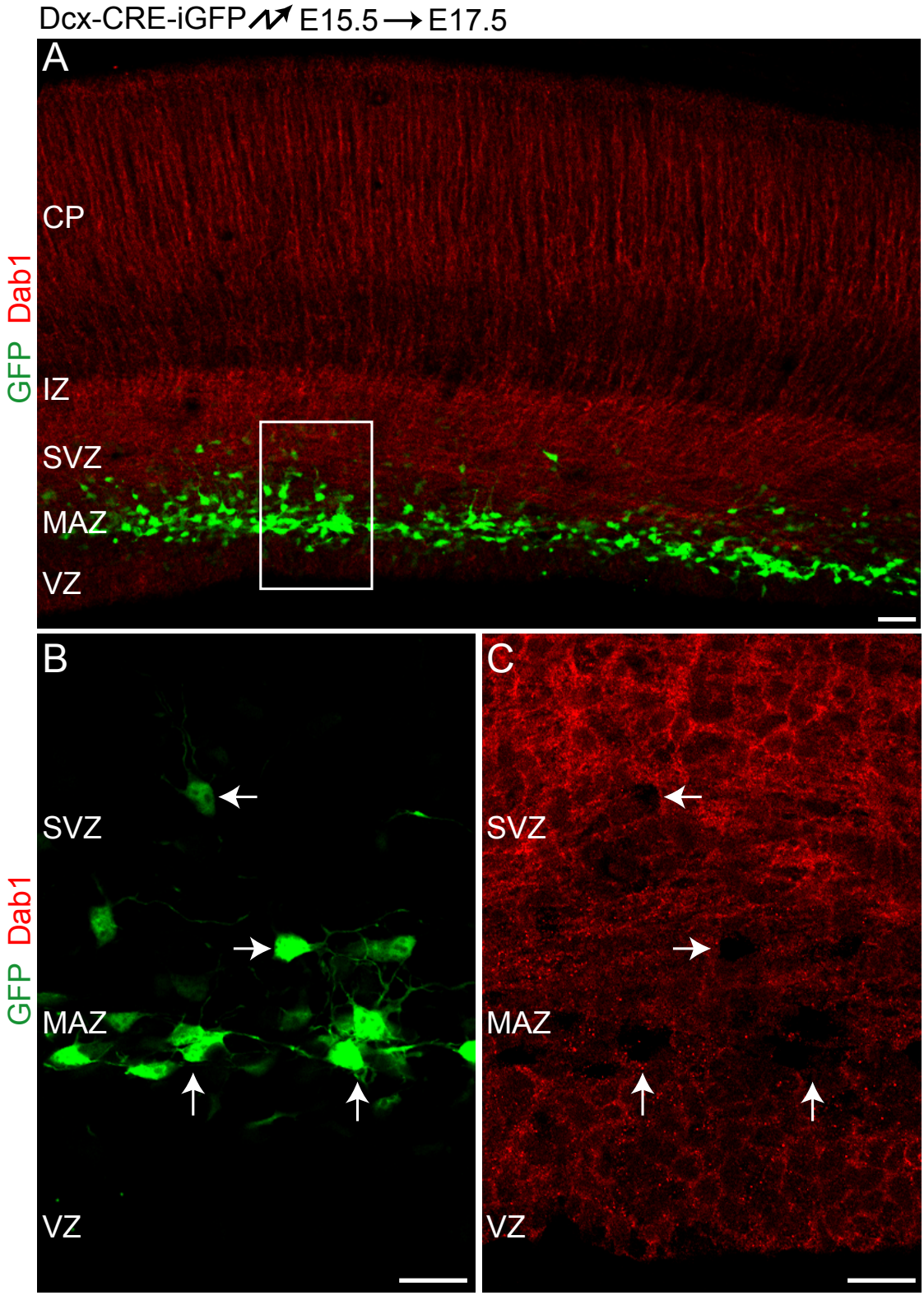

Figure S2. Loss of Dab1 protein after in utero electroporation of Dcx-CRE-iGFP into *Dab1-fl/fl* embryos. **(A)** Immunostaining for Dab1 two days (E17.5) after electroporation of Dcx-CRE-iGFP into *Dab1-fl/fl* embryos at E15.5. **(B-C)** High magnification single channel images of the boxed area shown in **(A)**. Arrows point to GFP-positive **(B)** electroporated cells that have decreased Dab1 immunoreactivity **(C)** compared to surrounding, untransfected cells. Scale bars represent 100 μm **(A)** and 50 μm **(B-C)**.

Figure S3, related to Figure 3 (Franco, et. al.)

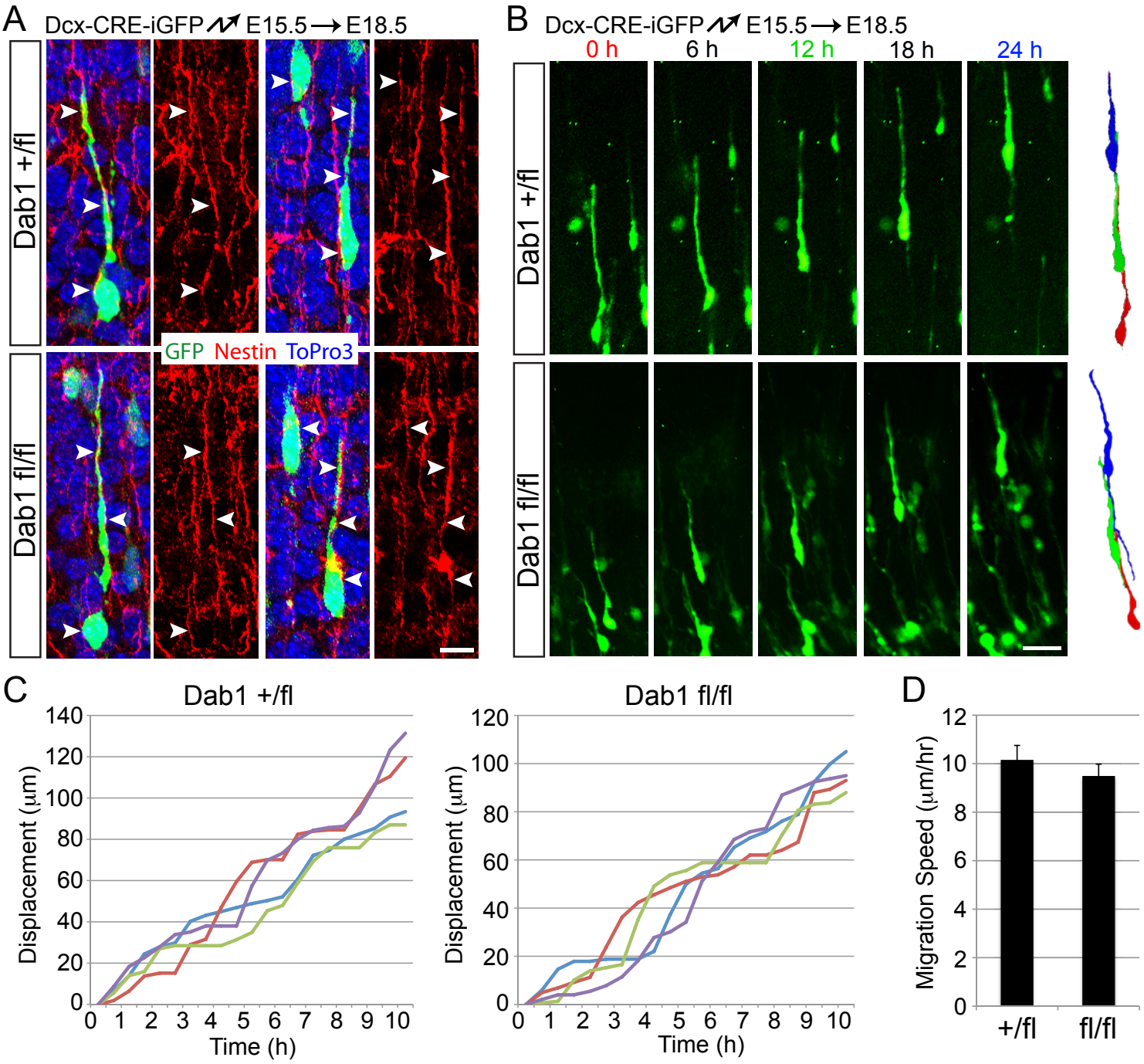

Figure S3. Dab1 is not required for glia-guided locomotion. **(A)** Normal neuron-glia interactions of Dab1-deficient neurons. Coronal sections from heterozygous (top panels) and homozygous (bottom panels) Dab1-flox embryos electroporated with Dcx-CRE-iGFP at E15.5 and analyzed at E18.5. Immunostaining for nestin shows electroporated neurons (green) in close apposition to nestin-positive RGC fibers (red) in the IZ (left panels) and CP (right panels) in control and mutant brains. **(B-D)** Glia-guided locomotion is unaffected by loss of Dab1. *Dab1+/fl* and *Dab1fl/fl* embryos were electroporated with Dcx-CRE-iGFP at E15.5, processed for slice cultures at E18.5, and imaged by spinning-disk confocal time-lapse microscopy. **(B)** Representative images from time-lapse experiments tracking the motility of electroporated neurons during glia-guided locomotion through the lower CP. To the right of each series, traces represent the migrating neurons at 0 h (red), 12 h (green) and 24 h (blue). **(C)** Traces of 4 control (left) and mutant (right) neurons migrating by glia-guided locomotion over a 10 hour period. Control and mutant neurons display saltatory movement in the lower CP. **(D)** Quantification of average migration speed of neurons undergoing glia-guided locomotion; Control = 10.1 ± 3.2 [s.d.] µm/hr, Mutant = 9.5 ± 3.6 [s.d.] µm/hr; P = 0.39 by t-test. Scale bars: 10 µm **(A)** and 25 µm **(B)**.

Figure S4, related to Figure 5 (Franco, et. al.)

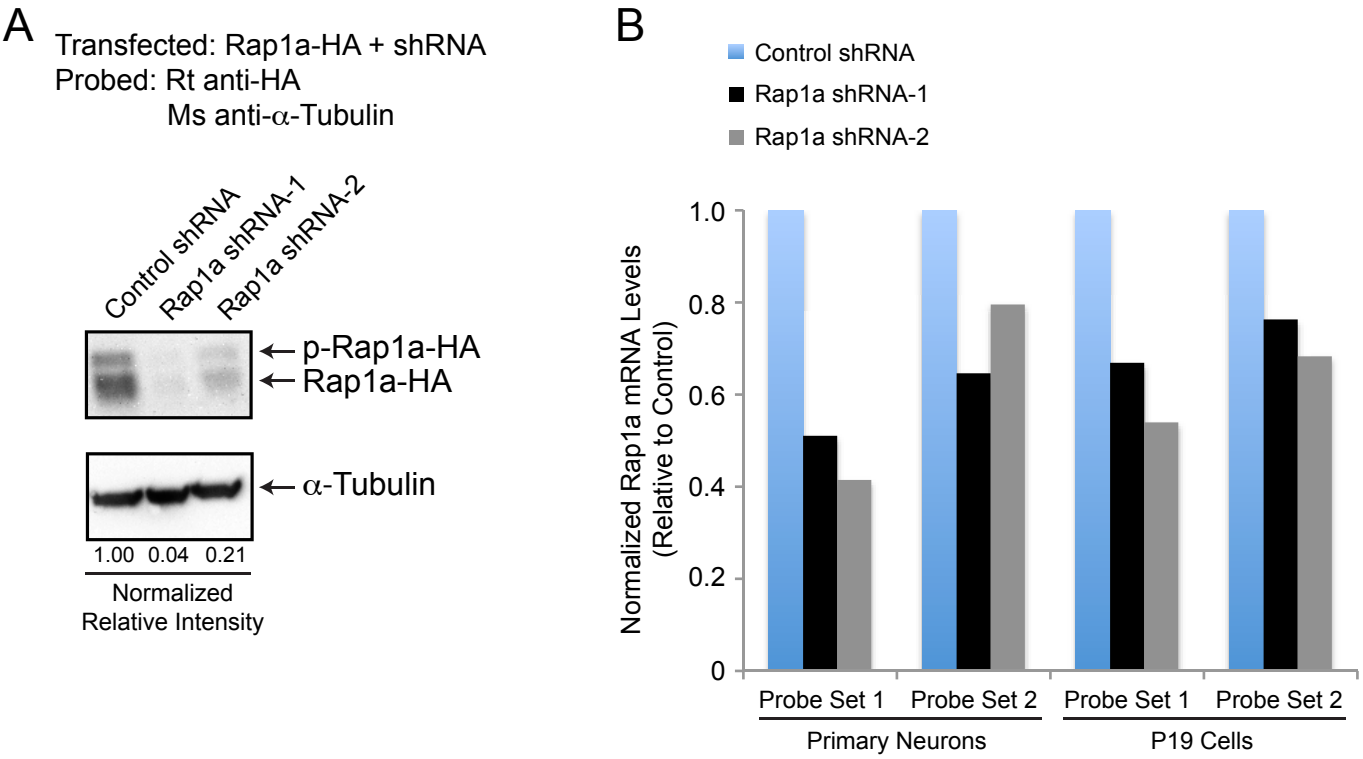

Figure S4. shRNA-mediated knockdown of Rap1a protein and mRNA. **(A)** Reduction of exogenously expressed Rap1a protein. Western blot showing reduction of HA-tagged Rap1a (Rap1a-HA) protein in lysates from 293T cells transfected with Rap1a-HA and shRNA constructs targeting mouse Rap1a, compared to lysates from cells transfected with Rap1a-HA and a non-silencing control shRNA. Blot was probed with anti-HA antibody followed by anti-α-tubulin as a loading control. Rap1a-HA signal was normalized to tubulin and quantified relative to control. **(B)** Reduction of endogenous Rap1a mRNA. Graph of quantitative RT-PCR results showing shRNA-mediated knockdown of endogenous Rap1a mRNA in primary neurons and P19 cells. Rap1a-specific or non-silencing control shRNAs were nucleofected into primary cortical neurons from E14.5 mouse embryos, or transfected into P19 cells, and RNA was harvested 48 hours later. Graph shows two different Rap1a-specific probe sets for each cell type. mRNA levels were normalized to a GAPDH control probe set and graphed relative to control shRNA samples.

Figure S5, related to Figure 6 (Franco, et. al.)

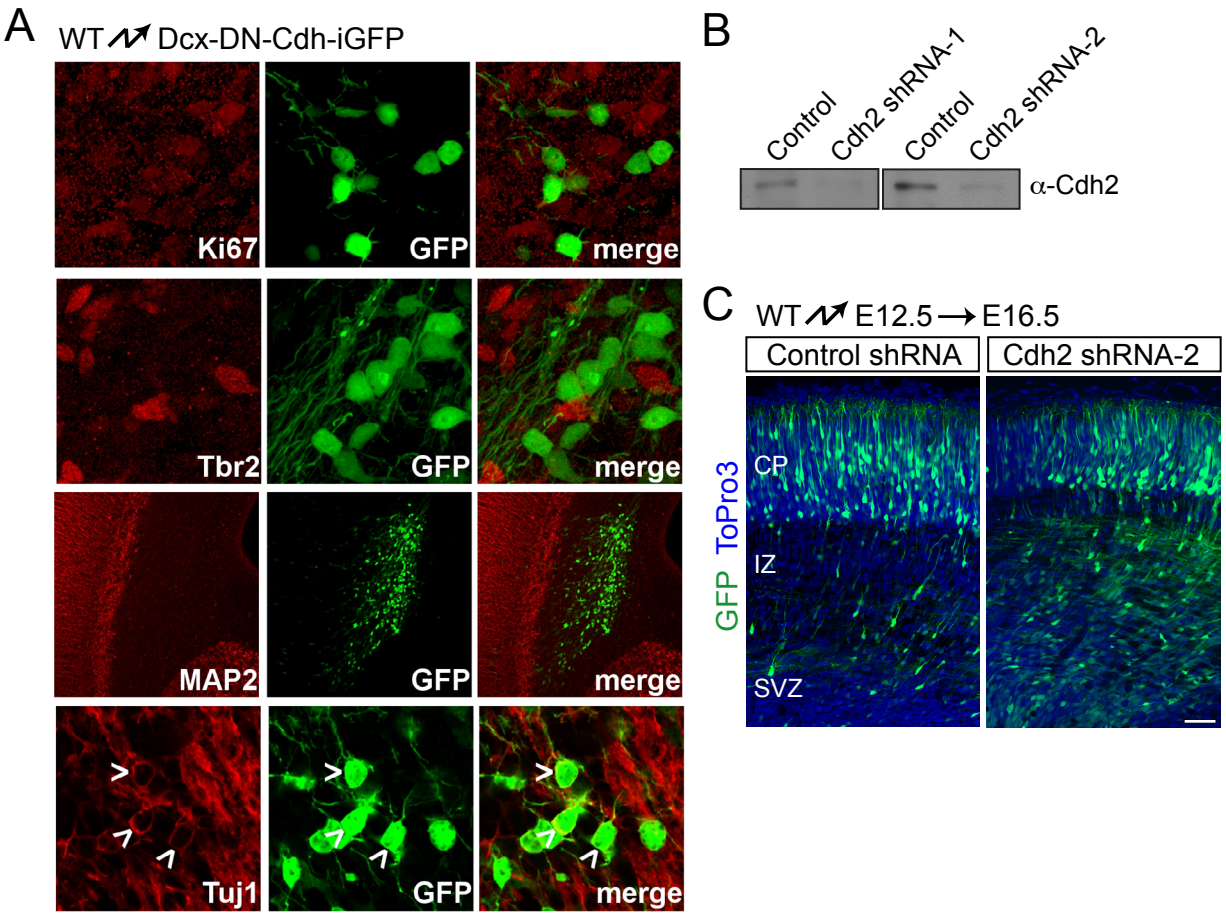

Figure S5. Controls for dominant-negative cadherin and Cdh2 shRNA. **(A)** DN-cadherin expressed from the Dcx promoter is expressed only in immature neurons. Dcx-DN-cadherin-iGFP was electroporated *in utero* and embryos were analyzed 2 days later. Immunohistochemical analysis revealed GFP+ cells were negative for Ki67, Tbr2 and Map2, demonstrating that electroporated cells were not proliferating, not intermediate progenitors and not mature neurons, respectively. Positive staining for Tuj1 (open arrowheads) shows that electroporated cells are immature neurons. **(B)** Reduction of Cdh2 protein by shRNA-mediated knockdown. Western blots probed with a Cdh2 antibody showing decreased Cdh2 protein levels after nucleofection of primary cortical neurons with either of two Cdh2-specific shRNA constructs. **(C)** Coronal sections from embryos electroporated at E12.5 with non-silencing control or an shRNA construct targeting Cdh2. Analysis performed at E16.5. Scale bar, 50 μm.

Figure S6, related to Figure 7 (Franco, et. al.)

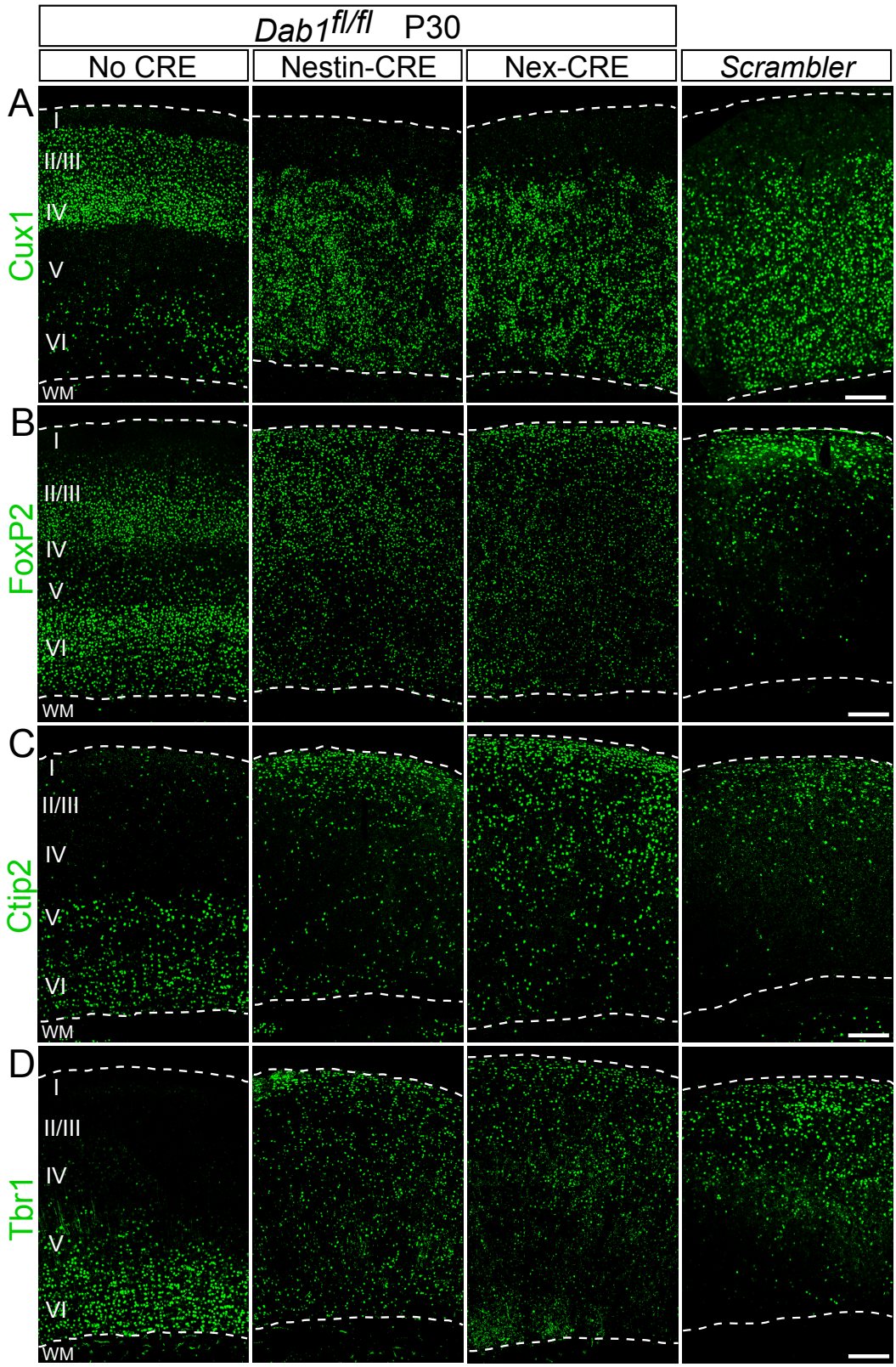

Figure S6. Similar neocortical lamination defects in *Dab1-NESTINko* and *Dab1-NEXko* mutant mice. (**A-D**) Immunostaining for neocortical layer markers at P30 in *Dab1fl/fl* (No CRE), *Dab1-NESTINko* (Nestin-CRE), *Dab1-NEXko* (Nex-CRE), and *Scrambler* mice. (**A**) Cux1 immunostaining reveals neurons that normally occupy layers II-IV. (**B**) FoxP2 stains primarily layer VI neurons and a subset of layer III/IV neurons. (**C**) Ctip2 labels neurons in layers V and VI. (**D**) Tbr1 stains layer VI neurons. Top dotted lines represent the pial surface and lower dotted lines outline the borders between layer VI and the white matter; ToPro3 counterstain (not shown) was used to identify these landmarks. Cortical layers are labeled I-VI. WM, white matter. Scale bars: 200 μm.

Figure S7, related to Figure 8 (Franco, et. al.)

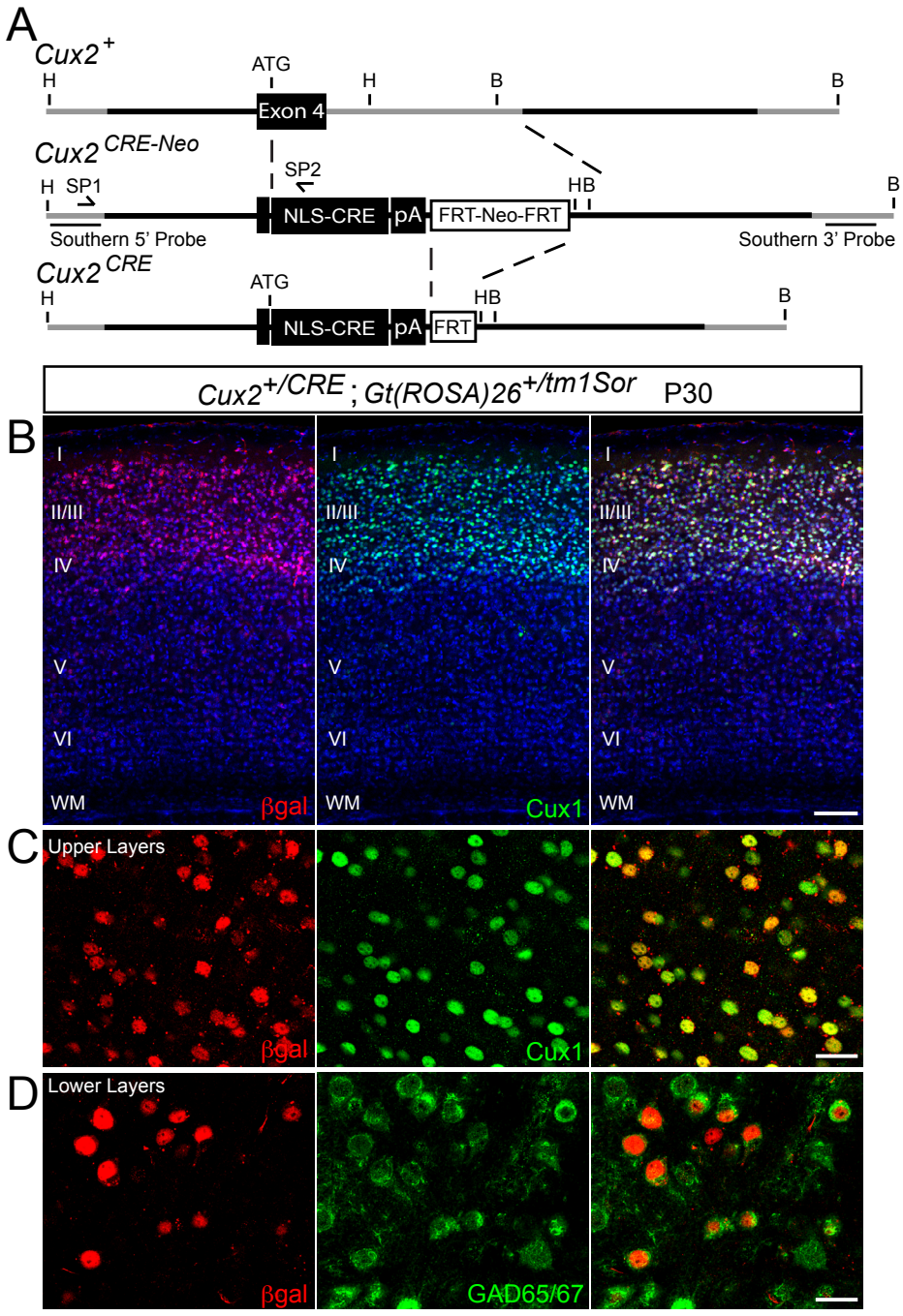

Figure S7. Generation and characterization of *Cux2-CRE* mice. **(A)** Schematic diagram of wild-type (+) and CRE (*CRE-Neo, CRE*) alleles of the *Cux2* gene. Thick black bars represent DNA segments used for constructing the targeting vector; gray bars identify flanking genomic DNA. Relevant restriction sites (B, BamHI; H, HindIII), Southern probes (thin black bars) and PCR primers for screening (SP1, SP2) and genotyping (GP1, GP2) are indicated. **(B)** CRE-mediated recombination in upper-layer neurons in *Cux2-CRE* mice. *Cux2-CRE* mice were mated to the *Rosa26R* LacZ reporter strain and analyzed at P30. Immunostaining for βgal (red) and Cux1 (green) demonstrates overlap of the two labels in neurons in layers II-IV. **(C)** High magnification of the upper-layer region of the cortical wall as stained in **(B)** shows expression of βgal (red) exclusively in Cux1-positive neurons (green). **(D)** High magnification of the lower-layer region of the cortical wall as stained in **(B)** demonstrates that the scattered βgal (red) labeling in deep layers is confined primarily to Gad65/67-positive interneurons (green). I, layer I; II/III, layers II-III; IV, layer IV; V, layer V; VI, layer VI; WM, white matter. Scale bars represent 1000 μm **(B)** and 50 μm **(C-D)**.

SUPPLEMENTAL EXPERIMENTAL PROCEDURES

Generation of mice. Gene-targeting was carried out using homologous recombination in embryonic stem cells. A *Dab1* gene-targeting vector was designed to insert LoxP sites flanking exon 2 of the *Dab1* gene, followed by a neomycin-resistance cassette (*PGK-neo*) flanked by two FRT sites. The vector was electroporated into 129P2/OlaHsd-derived E14TG2a embryonic stem (ES) cells and targeted ES cell clones were screened by PCR for targeting of the 3' arm (SP1: 5'-CTCTGGGGTTCGAATAAAG-3'; SP2: 5'-CATACGCTTGTGGTCCTATAC-3'). Positive clones were subsequently analyzed by Southern blot to confirm recombination of the 5' and 3' arms and to detect the presence of the 5' LoxP site (using HindIII digest of ES cell genomic DNA and the outside probes shown in Figure S1A). 2 confirmed clones were injected into C57BL/6J blastocysts and the resulting chimeras were then mated to C57BL/6J females to obtain germ-line transmission. Heterozygous F1 mice ($Dab1^{flox\text{-}neo/+}$) were mated with *B6.Cg-Tg(ACTFLPe)* mice (The Jackson Laboratory, Stock # 005703) to remove the *PGK-neo* cassette and the resulting offspring were subsequently mated to C57BL/6J mice to remove the *FLPe* transgene. Crossing heterozygous mice generated $Dab1^{flox/flox}$ mice and genotyping was performed by PCR (GP1: 5'-GGTTCAGTGCCTATCATGTATC-3'; GP2: 5'-GAGCCAGTGAGCGGTTCC-3') on tail DNA. $Dab1^{flox/flox}$ mice were mated to *Nestin-CRE* transgenic mice (Graus-Porta et al., 2001) and *Nex-CRE* mice (Belvindrah et al., 2007; Goebbels et al., 2006), which were genotyped as previously described (Goebbels et al., 2006; Graus-Porta et al., 2001). Double

heterozygous *Dab1*$^{flox/+}$*; Nestin-CRE* and *Dab1*$^{flox/+}$*; Nex-CRE* mice were crossed with homozygous *Dab1*$^{flox/flox}$ mice to obtain animals used in experiments.

The Cux2 gene-targeting vector was designed to insert the gene encoding CRE recombinase (CRE) into the endogenous translation start site in exon 4 of the *Cux2* gene. A PGK-neo cassette flanked by two FRT sites was included for negative selection. Gene targeting was performed at InGenious Targeting Laboratory, Inc. (Stony Brook, NY) by electroporation into C57BL/6-derived ES cells. Clones were screened by PCR for targeting of the 5' arm (SP3: 5'-AGAAGTCTCGGGGAAGCGTAAC-3'; SP4: 5'-ACCATTTCCGGTTATTCAACTT-3'). Positive clones were subsequently analyzed by Southern blot to confirm recombination of the 5' and 3' arms (using HindIII or BamHI digests of ES cell genomic DNA and the outside probes shown in Figure S7A) and by PCR (Cre1: 5'-GACATGTTCAGGGATCGCCAGGCG-3'; Cre2: 5'-GACGGAAATCCATCGCTCGACCAG-3') to confirm the presence of the CRE gene. 2 confirmed clones were injected into C57BL/6J-Tyr c-2J blastocysts and the resulting chimeras were then mated to C57BL/6J-Tyr c-2J females to obtain germ-line transmission. Breeding of F1 and F2 progeny was performed as described above and offspring were genotyped with primers Cre1 and Cre2. *Cux2*$^{cre/+}$ mice were mated to *Dab1*$^{flox/flox}$ mice to generate double heterozygous *Dab1*$^{flox/+}$*;Cux2* $^{CRE/+}$ mice, which were then crossed to *Dab1*$^{flox/flox}$ mice to obtain animals used in experiments. For staging of mice, midday of the day of the vaginal plug was considered as E0.5 and the day of birth was termed P0.

Expression Constructs. A segment of the mouse genomic region containing a promoter fragment from the *Dcx* gene was amplified by PCR (Dcx1: 5'-GTGCCACTTTTCAATTCCAGCCTTCAT-3'; Dcx2: 5'-AGTAACGGTCCCCATTGCGGTAGAA-3') and cloned as a BglII-XbaI fragment into pBluescriptII-SK+. A subfragment (SpeI-PflMI) was then cloned into a vector containing an internal ribosome entry site (IRES) and EGFP. Coding sequences for the following genes were inserted between the Dcx promoter and IRES-EGFP: NLS-CRE (Lewandoski et al., 1997), LIMK1-D460N (Edwards and Gill, 1999), Cofilin-S3A (Nagaoka et al., 1996), Akt1-K179M (Addgene plasmid 16243) (Franke et al., 1995) Rap1GAP (Han et al., 2006), Cdh2, DN-Cadherin (cytoplasmic domain of classical cadherins). Oligonucleotides containing the HA-tag sequence were ordered and cloned into pcDNA3 to create pcDNA-HA. Rap1a was amplified by PCR from E15.5 mouse brain cDNA (Rap1a-Hind-F 5'-CGTAAGCTTAGAGCGCATCATGCGTGAGTACAAG-3'; Rap1aEcoRV-R 5'-ATCCGATATCGAGCAGCAAACATGATTTCTTTTTAG-3') and cloned into pcDNA-HA. Rap1a shRNA expression vectors were purchased from Open Biosystems (TRCN0000055268 and TRCN0000055272). Cdh2 shRNAs (target sequences 5'-GACGGTCACTGCCATTGAT-3' and 5'-GCAAATCTATTTACTTGAT-3') were synthesized as oligonucleotides and cloned into a U6 promoter-containing vector.

Histology, Immunostaining and Immunoblotting. Nissl staining, immunohistological analysis and immunoblotting were performed essentially as

described (Belvindrah et al., 2007). Sections used for immunostaining were first subjected to antigen retrieval by boiling in citrate buffer. Antibodies used for immunostaining were as follows: anti-200kD Neurofilament Heavy (Smi-32) mouse monoclonal (1:2000; Abcam), anti-Chondroitin Sulfate (CS-56) mouse monoclonal (1:100; Sigma), anti-Ctip2 (25B6) rat monoclonal (1:500; Abcam), anti-Cux1 CDP (M-222) rabbit polyclonal (1:200; Santa Cruz Biotechnology), anti-Dab1 B3 rabbit polyclonal (1:400; kindly provided by J. Cooper, Fred Hutchinson Cancer Research Center), anti-FoxP2 rabbit polyclonal (1:500; Abcam), anti-GAD65/67 (1:1000; Sigma), anti-GM130 mouse monoclonal (1:250; BD Transduction Laboratories), anti-Map2 rabbit polyclonal (1:2000, kindly provided by S. Halpain, University of California – San Diego), anti-Tbr1 rabbit polyclonal (1:500; Abcam), anti-βgal (1:1000; Promega), anti-pan Cadherin (1:200; Abcam). Nuclei were stained with ToPro3 (1:10,000; Molecular Probes) and sections were mounted on slides with Prolong Gold mounting medium (Molecular Probes). Images were captured using a Fluoview FV500 (Olympus) laser-scanning confocal microscope. Image analysis and quantification was performed using MetaMorph software (Molecular Devices).

For immunoblotting from tissue, one hemisphere of the neocortex was dissected from each embryo at E16.5 and snap-frozen on liquid N_2. Tissue was then homogenized in lysis buffer (50mM Tris-HCl pH 7.6, 500 mM NaCl, 0.1% SDS, 0.5% DOC, 1% Triton X-100, 0.5 mM $MgCl_2$, with Complete Protease Inhibitor Cocktail Tablets [Roche]) on ice for 10 minutes and clarified by centrifugation at

4°C for 25 minutes. Protein concentration was determined by BCA assay (Pierce) and 75 μg of total protein was loaded for each sample. Anti-Dab1 rabbit polyclonal antibody (1:1000; Chemicon) was used for immunoblotting.

For Cdh2 Western blot, primary cortical neurons were nucleofected (Lonza AG) with Cdh2 shRNAs or control shRNA and lysed after 48 hours. For each sample, 40 μg of total protein was loaded. Anti-Cdh2 rat monoclonal antibody was used for immunoblotting (1:500; clone MNCD2 developed by M. Takeichi and H. Matsunami, obtained from the Developmental Studies Hybridoma Bank developed under the auspices of the NICHD and maintained by The University of Iowa, Department of Biology, Iowa City, IA 52242).

For Rap1-HA Western blot, 293-T cells were transfected with Rap1a or control shRNAs and Rap1a-HA. After 48 hours, cells were lysed and 40 μg of total protein was loaded for each sample. Anti-HA rat monoclonal antibody (1:2000; Invitrogen, clone 3F10) was used for immunoblotting. Anti-α-tubulin (1:2500; Sigma) was used as a loading control.

Quantitative RT-PCR. Total RNA was isolated using the RETROScript Kit (Ambion). RNA (400 ng) was reverse transcribed to cDNA using the SuperScript III Reverse Transcriptase system (Invitrogen) and specific transcripts were quantitated by real-time PCR using Chromo4 (MJ Research), gene-specific primers, and the SYBR GREEN system (Applied Biosystems). Primer sequences

for the mouse Rap1a probe sets were: Set 1 (For – 5'-CCT ACA GAA AGC AAG TCG AGG T-3', Rev – 5'-CTG TAA ATT GCT CGG TTC CTG-3'), Set 2 (For – 5'-CAT CAT GCG TGA GTA CAA GCT A-3', Rev- 5'-TGA ACA AAC TGA ACT GTC AGA GC-3'). Relative mRNA levels for Rap1a were determined using the comparative threshold cycle method (Applied Biosystems, User Bulletin 2, 1997) and normalized to glyceraldehyde-3-phosphate dehydrogenase mRNA levels.

Electron Microscopy. Embryonic (E15.5) brains were immersion fixed in one of two fixative formulations; either 4% paraformaldehyde + 1.5% glutaraldehyde in 0.1M cacodylate buffer + 1mM $CaCl_2$ or 1% paraformaldehyde + 3% glutaraldehyde in 0.1M cacodylate buffer + 5mM $CaCl_2$. The brains were buffer washed and postfixed in 1% OsO4 in 0.1M cacodylate buffer with 0.75% potassium ferricyanide for 2 hours. Following a buffer wash, tissues were dehydrated in graded ethanol series and transitioned in propylene oxide before embedding in Embed 812 / Araldite (Electron Microscopy Sciences, Hatfield PA). Thick sections (1-2μm) were cut, mounted on glass slides and stained in toluidine blue for general assessment in the light microscope. Subsequently, 70nm thin sections were cut, mounted on copper slot grids coated with parlodion and stained with uranyl acetate and lead citrate for examination on a Philips CM100 electron microscope (FEI, Hillsbrough OR) at 80kv. Images were collected using a Megaview III ccd camera (Olympus Soft Imaging Solutions, Lakewood CO).

SUPPLEMENTAL REFERENCES

Belvindrah, R., Graus-Porta, D., Goebbels, S., Nave, K.A., and Muller, U. (2007). Beta1 integrins in radial glia but not in migrating neurons are essential for the formation of cell layers in the cerebral cortex. J Neurosci *27*, 13854-13865.

Edwards, D.C., and Gill, G.N. (1999). Structural features of LIM kinase that control effects on the actin cytoskeleton. J Biol Chem *274*, 11352-11361.

Franke, T.F., Yang, S.I., Chan, T.O., Datta, K., Kazlauskas, A., Morrison, D.K., Kaplan, D.R., and Tsichlis, P.N. (1995). The protein kinase encoded by the Akt proto-oncogene is a target of the PDGF-activated phosphatidylinositol 3-kinase. Cell *81*, 727-736.

Goebbels, S., Bormuth, I., Bode, U., Hermanson, O., Schwab, M.H., and Nave, K.A. (2006). Genetic targeting of principal neurons in neocortex and hippocampus of NEX-Cre mice. Genesis *44*, 611-621.

Graus-Porta, D., Blaess, S., Senften, M., Littlewood-Evans, A., Damsky, C., Huang, Z., Orban, P., Klein, R., Schittny, J.C., and Muller, U. (2001). Beta1-class integrins regulate the development of laminae and folia in the cerebral and cerebellar cortex. Neuron *31*, 367-379.

Han, J., Lim, C.J., Watanabe, N., Soriani, A., Ratnikov, B., Calderwood, D.A., Puzon-McLaughlin, W., Lafuente, E.M., Boussiotis, V.A., Shattil, S.J.*, et al.* (2006). Reconstructing and deconstructing agonist-induced activation of integrin alphaIIbbeta3. Curr Biol *16*, 1796-1806.

Lewandoski, M., Meyers, E.N., and Martin, G.R. (1997). Analysis of Fgf8 gene function in vertebrate development. Cold Spring Harb Symp Quant Biol *62*, 159-168.

Nagaoka, R., Abe, H., and Obinata, T. (1996). Site-directed mutagenesis of the phosphorylation site of cofilin: its role in cofilin-actin interaction and cytoplasmic localization. Cell Motil Cytoskeleton *35*, 200-209.